Optimisation of the control of Neoclassical Tearing Modes with ECCD in ASDEX Upgrade and ITER

M. Maraschek[1], G. Gantenbein[2], Q. Yu[1], H. Zohm[1], S.Günter[1], F. Leuterer[1], A. Manini[1], ECRH group, ASDEX Upgrade Team[1]

[1]*Max-Planck-Institut für Plasmaphysik, EURATOM Association, Garching, Germany*
[2]*Forschungszentrum Karlsruhe, Association EURATOM-FZK, IHM, D-76021 Karlsruhe, Germany*

The ECCD deposition width during NTM stabilisation experiments has been scanned over a wide range relative to the island width. The highest efficiency in terms of stabilisation and achievable β_N with suppressed NTM could be achieved with a narrow deposition with the highest current density I_{ECCD}/d. For a broad deposition no stabilisation could be achieved. However, the NTM could be stabilised with modulated broad ECCD, depositing only in the islands O-point.

Introduction Neoclassical Tearing Modes (NTMs) are of great concern for tokamak plasmas, in particular for ITER and a future fusion reactor, as the presence of a (3/2)-NTM reduces the achievable β_N by at least 10-20%. As the achievable fusion power is proportional to β_N^2 this is not tolerable.

Schemes for the stabilisation of NTMs by local co - Electron Cyclotron Current Drive (co-ECCD) with respect to the plasma current have been developed at various experiments [1–3] and established as a tool with feedback capabilities. Therefore in ITER a system with 24 MW ECCD power at 170 GHz has been foreseen for this purpose. Most of present experiments are performed with a fixed ECCD deposition width d, which is smaller than the marginal island size W_{marg}. For $W < W_{marg}$ an NTM naturally decays away and β_N can rise again independently of the NTM size. For ITER, the condition $d < W_{marg}$ is not necessarily fulfilled, and possible ways to reliably stabilise an NTM have to be developed for this purpose. The effect of the ratio d/W_{marg} has been investigated. The modulation of the ECCD depositing only power in the islands O-point is predicted to improve the efficiency of the stabilisation. This has been proved experimentally and is compared with predictions.

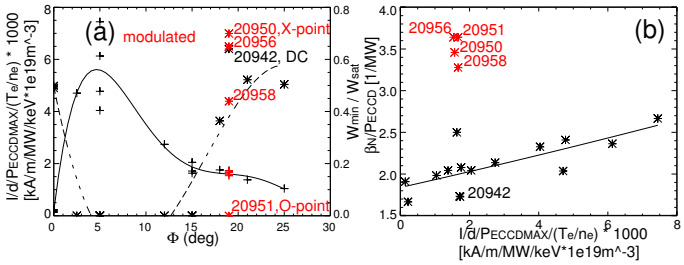

Figure 1: *TORBEAM calculations of the width and total driven current. The ratio $(I/d)/P_{ECCD}^{max}/(T_e/n_e)$ as function of the toroidal launching angle Φ (plus signs, solid curve) is shown in (a) together with the experimentally achieved reduction of the (3/2)-NTM normalised to the island size without ECCD (stars, broken curve for unmodulated ECCD). (b) shows the achieved maximal β_N/P_{ECCD} as function of $(I/d)/P_{ECCD}^{max}/(T_e/n_e)$. In both figures the discharges with modulated ECCD are added in red.*

Scan of the deposition width The deposition width and the driven current of the ECCD mainly depend on the toroidal launching angle of the ECCD mirror ($|\Phi| > 0°$ for co-ECCD, $\Phi = 0°$ for pure heating). With the toroidal magnetic field B_t and the poloidal launching angle Θ the major radius R_{dep} of the ECRH deposition and the resonant surface can be controlled, respectively. Only B_t can be varied during the discharge, whereas Θ has to be fixed beforehand and at present can not be changed during the discharge at ASDEX Upgrade. Presently 3 gyrotrons with approximately 400kW each, with independent mirrors are available. Typically Θ is adjusted in a way that the wave propagates through the plasma centre towards the deposition location on the high field side. The resonant surface is reached by a preprogrammed small scan of the magnetic field $B_t \approx -2.0T ... -2.3T$ towards higher absolute field. Based on TORBEAM calculations [4] the resulting deposition width d, current density j_{ECCD}, the total driven current I_{ECCD} and the resulting current peaking I_{ECCD}/d are calculated and shown in figure 1a. The current peaking is normalised to the maximal applied ECCD power P_{ECCD}^{max} and the ratio T_e/n_e in order to remove a variation in the driven current caused by different ECCD powers and different current drive efficiencies due to local plasma parameters.

From the calculations it can be seen that for a range $\Phi \approx 2°...8°$ the highest current density and hence

the highest I_{ECCD}/d are reached. Additionally the measured island size reduction $W_{min}/W_{sat}(noECCD)$ is shown. For pure heating ($\Phi = 0°$) and broad deposition with low I_{ECCD}/d ($\Phi \gtrsim 15°$) no complete stabilisation with unmodulated ECCD, but only a reduction to typically half the saturated island size is achieved (figure 1a). Only in the range $0° > \Phi \gtrsim 15°$ a complete stabilisation is possible.

Considering the achievable β_N for a given p_{ECCD} figure 1b (black points) shows β_N/P_{ECCD} as function of $(I_{ECCD}/d)/P^{max}_{ECCD}/(T_e/n_e)$. It can be clearly seen in the data points for unmodulated ECCD and in the corresponding linear fit, that with increasing current peaking $(I_{ECCD}/d)/P^{max}_{ECCD}/(T_e/n_e)$ (current density j_{ECCD}) the stabilisation gets more efficient and a higher β_N can be reached. The narrow deposition has been applied for the stabilisation of (3/2)-NTMs in improved H-mode discharges, where the NTM could be stabilised at the highest $\beta_N \approx 2.5$ at the lowest $q_{95} = 2.9$ at ASDEX Upgrade to date. This is below the ITER target value of $q_{95} = 3.0$.

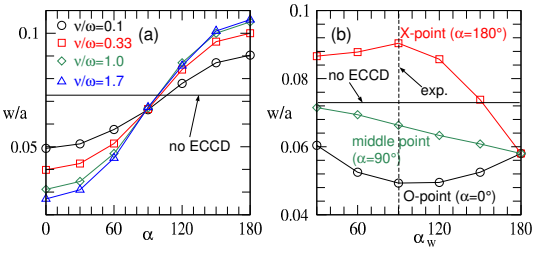

Figure 2: *(a) Variation of the island size with modulated ECCD (50% duty cycle) for different phasings ($\alpha = 0°$ for O-point, $\alpha = 180°$ for X-point). The current drive efficiency is included by different normalised fast electron collisionalities ν/ω indicated with different colours and symbols. (b) For $\alpha = 0°, 90°, 180°$ a variation of the duty cycle from a short ECCD pulse ($\alpha_w \to 0°$) to continuous ECCD ($\alpha_w = 180°$) has been calculated. Experiments were performed with $\alpha_w = 90°$.*

Theoretical predictions for broad ECCD deposition First theoretical considerations on the requirement of a modulation for NTM stabilisation assumed the deposition of the ECCD d to be smaller than the marginal island size W_{marg} [5]. With $d/W_{marg} < 1$ modulation does not improve the efficiency of the ECCD significantly and has been no longer considered [1,5,6]. The case presented above has $d/W_{marg} > 1$ and with the maximal ECCD power the (3/2)-NTM could be no longer stabilised. Calculations for $d/W_{marg} > 1$ show, that the efficiency of ECCD stabilisation is significantly improved with modulation in the O-point of the island [6].

Calculations on the effect of the different phasings and duty cycles have been performed in order to gain a full understanding of the experimental findings. A deposition width of 20% of the minor plasma radius, i.e. $d/a = 0.2$, has been assumed. The phase angle α and α_w in figure 2 correspond to the phasing and the duty cycle of the ECCD, respectively. The considered model presently ignores the heating effect on the stabilisation efficiency [6]. The effect of the fast electron collisionality is included, which governs the time it takes to build up the current in the O-point. Values of $\nu \cdot \tau_R = 3 \cdot 10^3, 1 \cdot 10^4, 3 \cdot 10^4, 5 \cdot 10^4$ have been used, corresponding to $\nu/\omega = 0.1, 0.33, 1.0, 1.7$, with ω representing the angular frequency of the mode and $\tau_R = a^2\mu_0/\eta$ the resistive time scale. For $\nu/\omega << 1$ it takes several tens of oscillations until the time averaged saturated ECCD current is reached. This is consistent with the increasing effect of the modulated ECCD with increasing ν/ω (figure 2a). For O and X-point phasing a stabilising and destabilising effects are predicted, respectively. A duty cycle of 50% is predicted to have the strongest effect for both phasings.

Modulated ECCD with broad deposition As shown above, with a broad ECCD deposition ($\Phi > 15°$) the NTM can not be stabilised completely and the achievable β_N/P_{ECCD} is reduced. By applying broad modulated ECCD with power deposition only in or near the islands O-point, a complete stabilisation can be regained (figure 3, #20951). A recovery to $\beta_N = 2.0$ at $q_{95} \approx 4.9$ could be achieved.

A direct comparison between 2 identical discharges clearly shows the improvement with O-point modulation (figure 3). In both cases the mode amplitude is initially reduced during the B_t-ramp when the ECCD moves radially into the island, but only in the modulated case the mode disappears and β_N recovers. In the unmodulated case β_N stays at values comparable to the time when the ECCD has not yet reached the resonant surface.

The data points for the modulated broad ECCD deposition are added in the diagrams in figure 1 in red. The current peaking is comparable to the unmodulated cases with $\nu/\omega \geq 1$ assumed. The island size reduction for $\Phi = 19°$ shows a variation from complete stabilisation for #20951 to worse stabilisation than for the unmodulated case #20942 (see next section). The improvement in β_N/P_{ECCD} in figure

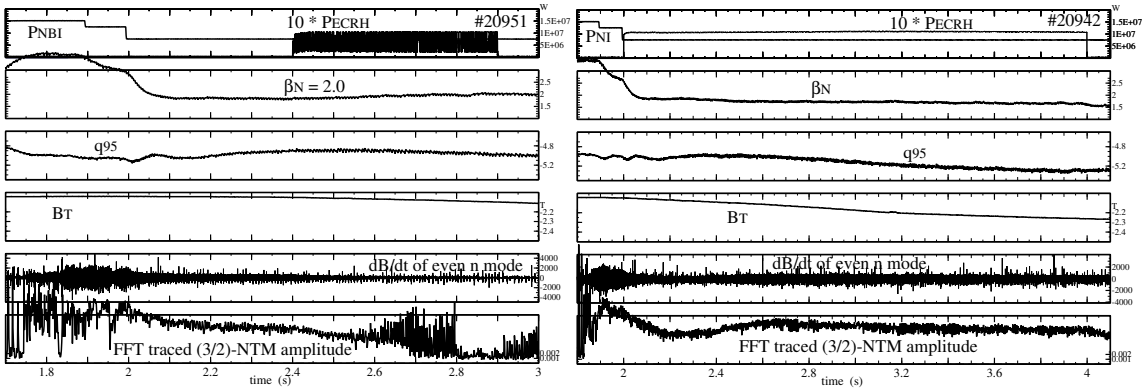

Figure 3: *Stabilisation of a (3/2)-NTM in discharge #20951 with broad and modulated ECCD in the O-point of the island. The time traces show the heating power (P_{NBI} and the modulated P_{ECCD}), β_N, q_{95}, the preprogrammed ramped B_t for the resonance scan, the dB_{pol}/dt raw data and the FFT traced island amplitude of the (3/2)-NTM. A complete stabilisation can be observed after 2.7s. Discharge #20942 is identical, but unmodulated ECCD has been used, and the mode could not be stabilised.*

1b shows two distinct groups for unmodulated and modulated discharges. For the unmodulated cases an improvement with increasing current peaking can be seen. For the modulated cases much higher values in β_N/P_{ECCD} can be observed. This is dominantly due to the halved average ECCD power to reach the same β_N. At present no deposition width scan has been performed for the modulated cases.

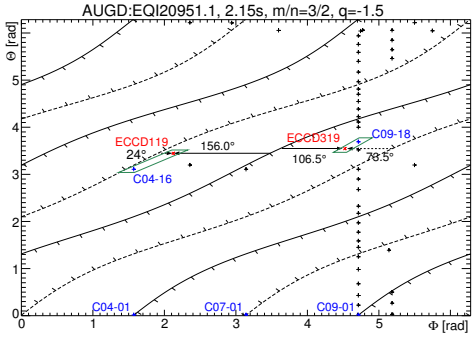

Figure 4: *Mapping between the location of the ECCD deposition ($\times$ signs) from TORBEAM calculations and the location of the Mirnov probes ($+$ signs) considering the straight field line angle. The phase is adjusted to the location of the reference coils (C09-01 + C04-01). An additional phase check with the probes C04-16 and C09-18 for gyrotron 1 and 3,4, respectively, is possible.*

Effect of the phasing of modulated ECCD In order to resolve the influence of the relative phase between the islands O-point and the deposited ECCD power, the ECCD has been modulated with different phases. The phase of the mode has been determined by a combination of Mirnov coils (measuring dB_{pol}/dt). This phase has to be mapped along the magnetic field line on the $q = m/n = 1.5$ resonant surface. One has to take the poloidally varying field line angle into account by using the so called straight field line angle $\Theta^*(\Theta)$. In the $\Theta^*(\Theta) - \Phi$ plane field lines appear as straight lines and consequently the expected phase at the measurement positions can be reconstructed for arbitrary plasma shapes. In figure 4 the mapping between the reference coils and gyrotrons 1 and 3+4 is shown. For the modulation of the ECCD the sum of the signal of the two coils C09-01 and C04-01 has been used. They are located 180° toroidally apart. A precalculated phase shift for each gyrotron has been included taking into account the phase difference between the magnetic field line and the calculated ECCD deposition.

Based on the field line mapping the alignment of the ECCD deposition with the island can be compared with a subset of coils lying on the same magnetic field line as the ECCD deposition, as indicated in figure 5a (coil C04-16 for gyrotron 1 and coil C09-18 for gyrotrons 3 and 4). For both groups of gyrotrons and all coils the gyrotrons are injecting ECCD power mainly during the time interval with $B_{pol}^{island} < 0$ ($d(dB_{pol}^{island}/dt)/dt > 0$). As the perturbation current within the island j_{island} flows parallel to the plasma current I_p in the X-point and antiparallel in the O-point, it becomes clear that the ECCD is deposited in phase with the islands O-point in discharge #20951 (figure 5a). The perturbation field B_{pol}^{island} has the same sign as the field from the plasma current B_{pol}^{plasma} at the X-point and the opposite sign at the O-point.